CHAPTER 6:

CU DEPOSITION ON THYMINE / ADENINE MODIFIED AU(111)

It is well known that the metal deposition is strongly influenced by organic molecules. Organic molecules are often used in galvanotechnique to produce smooth, mirror-like metal deposits. The mechanism of action of the organic molecules is often unknown and the processes employed were found in an empirical way. To enlighten the first stages of metal deposition on adsorbate-modified electrodes is therefore one of the starting steps to elucidate the action of organic molecules and to make predictions for the effects of definite classes of organic molecules in these processes.

6.1 Cu Deposition on Thymine modified Au(111)

To provide a contribution to this field we present the copper deposition on thymine modified Au(111) electrodes. This system was chosen because both separate systems, the copper deposition as well as the thymine adsorption on Au(111), are very well analyzed by numerous *ex situ* and *in situ* methods [118, 129, 131, 161, 162]. Additionally, one gets information about the interaction between different metals and DNA bases in an aqueous environment depending on the orientation of the molecules, the discharging state of the metal ions and the electrode potential.

Thymine represents a well investigated system at gold single crystal electrodes. Depending on the potential, two different, well-ordered adsorption layers can be recognized on Au(111) electrode. Negative of the PZC, a first order phase transition takes place in which randomly adsorbed thymine molecules form an ordered, physisorbed condensed state. The plane of thymine molecules is oriented nearly parallel to the electrode. In the potential region positive of the PZC the physisorbed monolayer is transformed into a chemisorbed adsorption state of thymine.

Exactly in the potential region where thymine is physisorbed, the UPD of copper takes place (Fig. 6.1). In the present study, the electrolyte contains beside thymine and copper ions only perchlorate anions to exclude any side effects by coadsorbing anions. At the adjusted pH value 1, thymine molecules are mostly available in the neutral state.
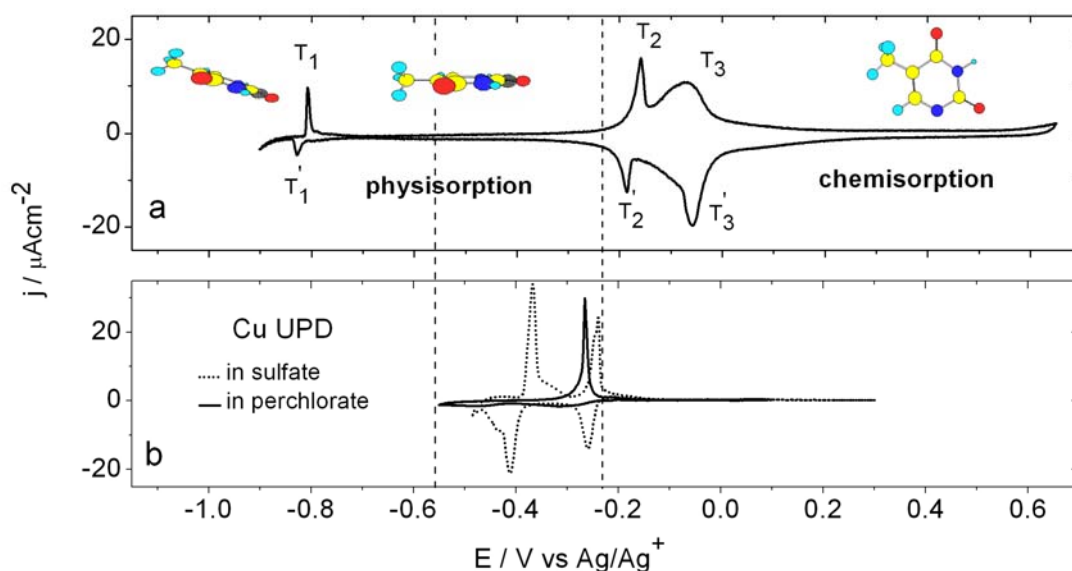
Figure 6.1: *The cyclic voltammograms of a) 12 mM Thymine + 0.1 M HClO₄ + 0.060 M NaClO₄. Sweep rate: 50 mV/s. b) 1 mM CuSO₄ + 0.1 M HClO₄ + 0.020 M Na₂SO₄ (dashed line), 1 mM Cu(ClO₄)₂ + 0.1 M HClO₄ + 0.060 M NaClO₄ (solid line) on Au(111). Sweep rates: 5 mV/s.*

We have investigated the copper deposition on the Au(111) electrode at two different bulk concentrations of thymine (1 and 12 mM). We already know that at a concentration of 12 mM physisorbed thymine molecules form condensed hydrogen bonded network. At low bulk concentration of thymine (1 mM), it occurs in negligible degree. The following voltammograms (Fig. 6.2.a-c) taken at 50, 5 and 2 mV/s scan rates show the adsorption behavior of Cu deposition on thymine modified Au(111) electrode.
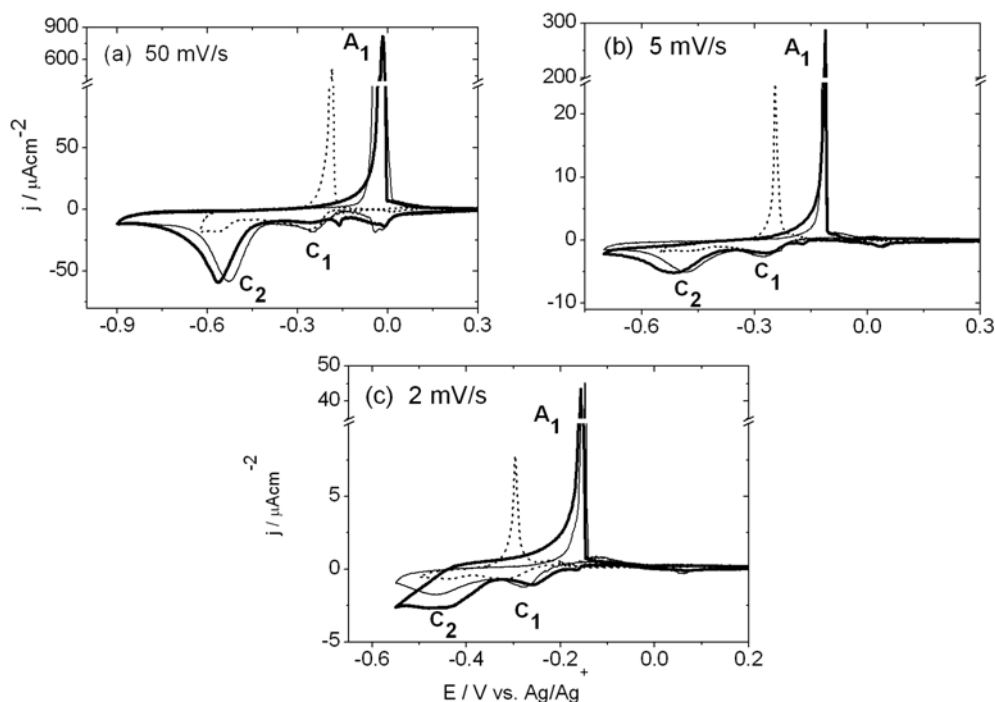
Figure 6.2: *Cyclic voltammograms of copper [1 mM Cu(ClO$_4$)$_2$, without thymine (dashed lines)] deposition on Au(111) in 0.1 M HClO$_4$ + 0.060 M NaClO$_4$ electrolytes. 1 mM thymine (thin lines), 12 mM thymine (thick lines). Scan rates: 50 (a), 5 mV/s (b), 2 mV/s (c).*

The cyclic voltammograms of Cu UPD on thymine modified Au(111) electrode show two adsorption peaks (C$_1$ and C$_2$) and a sharp stripping peak (A$_1$). The position of the first UPD peak (C$_1$) shows differences depending on the scan rate as well as the bulk concentrations of thymine; at higher scan rate (50 mV/s) and in the case of the higher concentration of thymine the first step is inhibited. However, interestingly at small scan rate (2 mV/s) as well as in the case of higher thymine concentration, UPD starts earlier compared to the copper UPD in thymine-free electrolyte and containing 1 mM thymine containing electrolyte.

The second step of copper UPD in thymine containing electrolyte exhibits an interesting consequence. The voltammograms scanned at different rates clearly indicate that the UPD of copper is amplified strongly by physisorbed thymine molecules. However, this effect is not still stronger than it is when using electrolytes containing sulphate anions. The peak position of C$_2$ in the electrolyte containing higher thymine concentration (12 mM) is located at more negative potentials at higher scan rates (50 and 5 mV/s). However, at the scan rate of 2 mV/s, the second step starts at more positive potential and is much greater than in solutions containing only 1 mM

thymine or no thymine. This shows that the higher thymine concentration promotes the Cu deposition.

The dissolution of the copper UPD layer is a one-step mechanism having a sharp stripping peak A_1. In thymine containing electrolytes, this peak is located at more positive potentials compared to the position in thymine-free electrolyte (even scanned to the same end potential in thymine-free electrolyte). This behavior indicates that thymine enhances the strength of interaction between the adsorbates (copper and/or thymine) and the surface gold atoms.

In contrast to the second step, at bulk potential region of copper, thymine acts as an inhibitor. Normally, the onset of bulk deposition in perchlorate solution is also at more negative potentials than the Nernst potential of Cu^0/Cu^{2+} (-0.49 V vs. Ag/Ag^+). However, in thymine containing electrolytes, bulk deposition of copper takes place more negative than that of perchlorate solution. Therefore, we have to consider two effects: the catalytical effect of adsorbed thymine on the copper UPD and the inhibition effect on the copper bulk deposition (OPD).

6.1.1 Chronocoulometry Experiments

To get an idea about the driving underlying processes causing the catalytical action of physisorbed thymine molecules to copper UPD, detailed chronocoulometric studies were performed according to the following potential sweep and step routine:

(1) Scanning from 0.3 V to the formation peak potentials (-0.465 V vs. Ag/Ag^+) with a scan rate of 2 mV/s and waiting there for different times (see Fig. 6.3.). The chosen formation (waiting) potentials are 25 mV positive of the Nernst potential of the Cu/Cu^{2+} couple to avoid the bulk deposition.

(2) Stepping from the formation peak potential into the dissolution potential (-0.1 V).
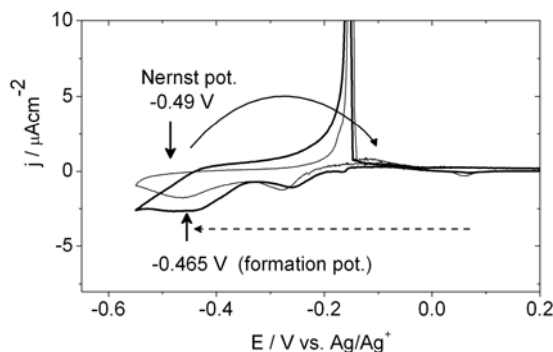
Figure 6.3: *Cyclic voltammograms on which the coulometric measurements are based in the electrolyte of 12 mM (thick line) and 1 mM thymine (thin line) containing 1 mM $Cu(ClO_4)_2$ + 0.1 M $HClO_4$ + 0.060 M $NaClO_4$. Sweep rates are 2 mV/s.*

For better understanding the influence of thymine, the chronocoulometric results from pure copper system in perchlorate solution are included.

6.1.1.a Formation Process

During the waiting time at the formation potential (peak potentials) the current-time evolution presented in Fig. 6.4 could be obtained. In a pure perchlorate solution the formation of the UPD layer is finished after about 27 min. This time-consuming process is the reason that in the voltammogram almost no charge flow can be recognized. But the higher the thymine concentration is, the faster is the deposition process. For 1 mM thymine concentration the formation process is finished after 4 min, for 12 mM thymine concentration after about 2 min. This was surprising because for the 12 mM thymine concentration a condensed adsorption layer is present at the surface. We expected therefore more an inhibition effect, which is however definitely not the case. Although the peak potentials differ slightly, so that an absolute comparison of the kinetics is difficult, this diagram clearly shows the active role of thymine molecules in the copper deposition process.
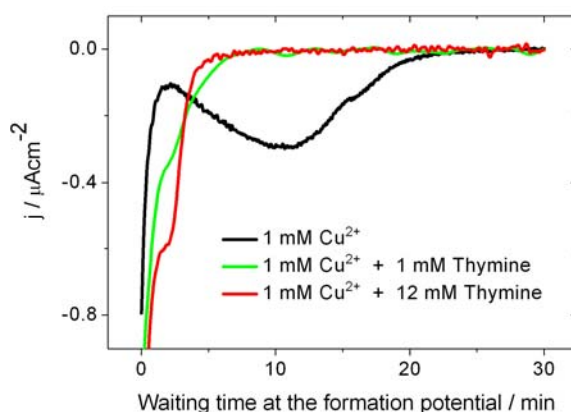

Figure 6.4 *Current-time transients measured at the formation potentials -0.465 V for copper and thymine containing solutions (1mM Thymine: green curve, 12 mM Thymine: red curve) and -0.44 V for pure copper solution (black curve).*

6.1.1.b   Dissolution process and Avrami analysis

In contrast to the long-time scale of the formation process, the dissolution of the formed structure is much faster and is finished on a second scale (Fig. 6.5.a-c). It is worth noting that the dissolution of copper-thymine adlayer (Fig. 6.5.b,c) takes longer times compared to that of a thymine-free copper adlayer. This is parallel to the result shown in the CVs (Fig. 6.2.c) (positons of stripping peaks locate at more positive potentials in thymine containing electrolyte). As conclusion, thymine leads to the stabilization of copper adatoms.

Beside this, the peak positions of the first dissolution transients (without waiting) shift to longer times with increasing thymine concentration. It reveals that the rate of formation of more stable adlayer depends on the bulk thymine concentration.

It is interesting to note that for all considered systems (pure perchlorate, 1 mM thymine, 12 mM thymine) the time needed for the dissolution jumps to longer times until the formation is completed. The dissolution of modified electrodes waiting 1 and 6 minutes in 1 mM and 12 mM thymine containing electrolyte, respectively, take place at the longest times. These two waiting times indicate the turning points corresponding to the formation of almost one monolayer. It tells us that the dissolution of a submonolayer of copper-thymine adlayer is energetically more favored compared to that of a full ML. In other word, stabilization of copper layer rises with coverage.
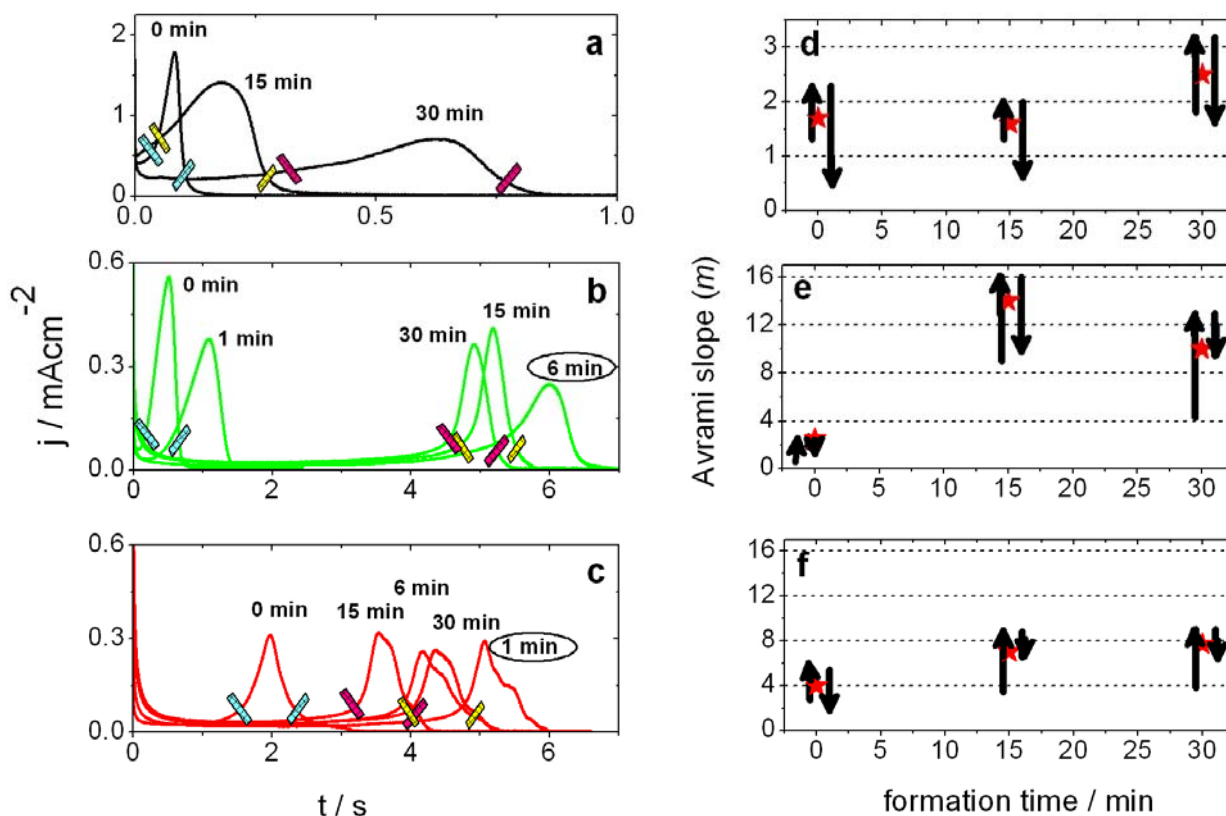
Figure 6.5: *Dissolution transients obtained after waiting (written on top of transients) at the formation potential of -0.465 V (-0.44 V for Copper alone) and stepping into the dissolution potential -0.1 V* **a:** *1 mM Cu(ClO$_4$)$_2$* (**black**), **b:** *1 mM thymine, 1 mM Cu(ClO$_4$)$_2$* (**green**), **c:** *12 mM thymine, 1 mM Cu(ClO$_4$)$_2$* (**red**). **d-f:** *The corresponding changes of Avrami slopes (stars point the slopes of the fit curves belonging to the entire Avrami plot).*

Avrami analysis

The shapes of transients (Fig. 6.5.a-c) obviously imply that the dissolution process obeys the hole nucleation and growth law. From the conventional point of view, it is very interesting that Avrami slope values climb to very high degrees in thymine containing electrolytes (Fig. 6.5.e,f) compared to those of thymine-free one (Fig. 6.5.d). Therefore, it can be concluded that the dissolution process occurring in thymine containing electrolytes obeys the power law nucleation combined with either surface diffusion or constant growth mechanisms from the conventional point of view.

The reason behind the extreme increase in Avrami slopes is the result of delaying of dissolution process (as the result of stabilizing role of thymine), i.e., shift of transients to longer times. Mathematically, the rate of natural logarithm "*ln*t" function increases slowly at longer "t" values (for example, 5-6 s), whereas, at smaller time values (for example, 0.1-1 s), the rate is higher. Due to Avrami slope is reversely proportional with the change of "*ln*t", those extreme values are observed.

From the predator-prey model point of view, the common feature of all Avrami curves analysed is the change of slope values. In other words, at the initial and at the final stages of transients the slope values are smaller compared to those of middle stage. It implies that the dissolution is slow at the middle stage of considered parts of transients. This behaviour was also observed in former analysed transients (see Section 5.3.2.a-b). Therefore, the same interpretation is also valid for the present case.

Charge density diagram

The integration of the dissolution current transients results in the charge–potential diagram shown in Fig. 6.6. The diagram of sulphate experiment (Fig. 5.4) is also included (full circle) for comparison.

It is obvious that thymine acts like sulphate anion in the UPD of copper. Reaching to the limiting charge value in the presence of 12 mM thymine or in sulphate containing electrolyte takes place in first minutes, whereas in a pure perchlorate solution the limiting value can be reached almost in half an hour. The charge value achieved in half an hour is 350 ± 5 μCcm^{-2} and 340 ± 5 μCcm^{-2} for a thymine modified electrode in 12 mM thymine and 1 mM thymine, respectively. The corresponding charge value for the Cu-UPD in SO_4^{2-} is also a close value, which is 340 ± 5. The formation of a fully discharged copper monolayer would consume 440 μCcm^{-2}. Our experimentally limiting found values differ, therefore, about 100 μCcm^{-2} from the theoretical one. The deficit in charge most likely come from the anion coadsorption leading some charge transfer as also proposed by Herrero et. al. [82].
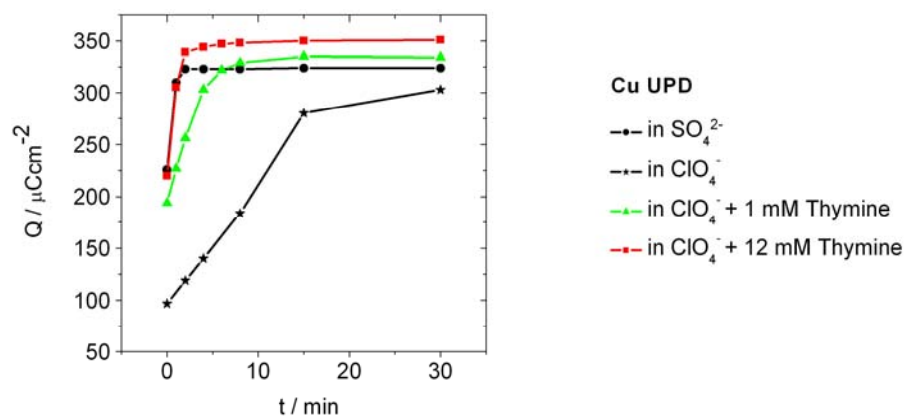
Figure 6.6: *Charge density-formation time diagram obtained after the integration of the dissolution transients.* ***Black:*** *Copper alone;* ***red:*** *12 mM thymine / copper;* ***green:*** *1 mM thymine / copper.*

6.1.2 STM study

In order to obtain some information about the copper-thymine structure on the Au(111) surface, C. Meyer carried out EC-STM experiments [7]. He investigated the copper deposition on thymine modified electrode at three different potentials:

At the first UPD region (-0.31 V), resolution of the STM pictures were possible only after 10 minutes. In these pictures thymine is oriented upright in contrast to the pure thymine system, for which in this region a flat orientation of thymine was resolved. It can be speculated that copper–thymine complexes are adsorbed at the Au(111) surface. As copper is not discharged at this potential, the complex is movable along the surface and the structure is mainly determined by the thymine stacking interaction more than by the underlying substrate.

At the second UPD region (-0.42 V), an upright orientation of thymine molecules were determined. The formed structure is similar to the one formed at positive potentials on bare Au(111). He proposed a model for adsorbed thymine molecules assuming that only every second copper row is covered by thymine molecules. Therefore, thymine is chemisorbed in the negative potential region on top of discharged copper adatoms.

6.1.3 XPS study

XPS measurements have been performed to analyze the chemical state of thymine on top of the copper adlayer on Au(111) surface at different conditions. The main objective was to

investigate the influence of thymine on the deposition of copper. It is clear that the emersed adlayer will not represent in every detail the adsorption structure in solution because the interfacial water and electrolyte will be removed upon rinsing and afterwards under vacuum conditions at 293 K.

We prepared samples in 12 mM thymine, 0.100 M $HClO_4$ and 0.060 M $NaClO_4$ electrolyte in the presence and absence of $Cu(ClO_4)_2$ (1 mM) as stated in the following routines. The preparation of the samples in the electrochemical cell and their transfer to the UHV chamber has been described in chapter 5 in detail.

The XPS survey spectra of copper-thymine deposited Au(111) electrodes are shown in Fig. 6.7. For comparison the spectrum II belonging to the underpotentially deposited copper in thymine-free electrolyte is included. The following routines were applied for each spectrum:

I: After waiting 10 minutes at -0.48 V representing the deposition at UPD region in 12 mM thymine and 1 mM $Cu(ClO_4)_2$, the probe has been emersed, rinsed with water and transferred to the UHV chamber.

II: After waiting waiting 30 minutes at -0.48 V representing the deposition at UPD region in 1 mM $Cu(ClO_4)_2$, the probe has been emersed, rinsed with water and transferred to the UHV chamber.
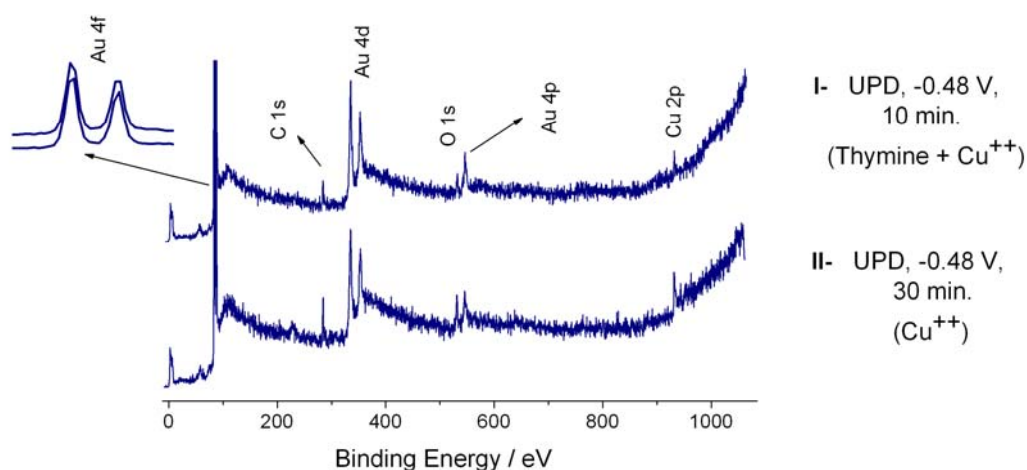

Figure 6.7: *The XPS survey spectra belong to the thymine-modified (I) and the unmodified (II) copper deposited Au(111).*

The survey spectra shown in Fig. 6.7 reflect no significant difference from each other. However, it is possible to differentiate some signals in the high-resolution XPS spectra. For a better interpretation, signals of Cu-2p, N-1s and C-1s core level will be shown below.

Cu-2p

The typical Cu-2p core level spectra taken from thymine-modified and unmodified copper deposited samples are shown in Fig 6.8 using excitation energies of 1150 eV. The spectrum belonging to the modified copper underpotential deposition exhibits some differences and similarities compared to the spectrum of unmodified one.
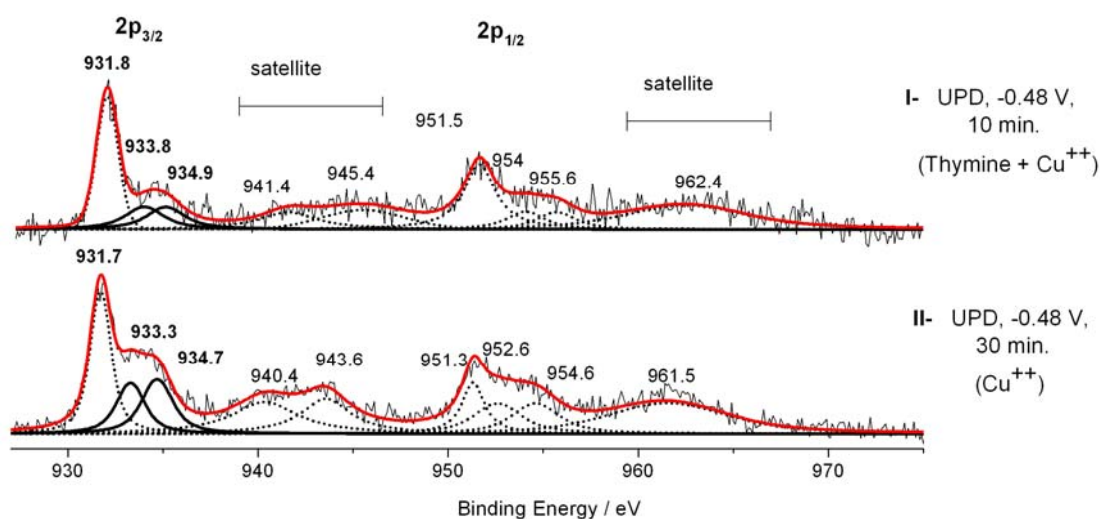
Figure 6.8: *XPS Cu-2p spectra of copper deposited on thymine modified (I) and unmodified Au(111) (II).*

One of the main differences is that the level of the oxidized copper is very low in thymine modified sample. Two indications; the first is the poor $2p_{3/2}$ signal around 934-935 eV and the second is the very weak satellite signals around 944.0 eV and 963.3 eV, prove this idea.

The intrinsic ratio of the $2p_{3/2}$ signals of the oxidized copper to the metallic copper (931.8 eV) have a ratio of 1:4 in the thymine containing sample (I). However, the corresponding ratio in the thymine-free sample (II) is 2:4. It should be remembered that the signals around at the BE of 934.0 have two components which are close to the values of 933.8 eV for CuO and 935.0 eV for $Cu(OH)_2$. The pH of the electrolyte, in which the probes have been produced, is about 1. After emersion of the electrode, the pH changes by rinsing with water. It cannot be excluded the

formation of CuO or Cu(OH)$_2$ by this procedure as well as transferring as discussed before (section 5.3.4). However, it is more probable that on the thymine modified probe a thymine complex of Cu^{2+} exists which may lead to the signal at 934-935 eV. On the other hand, the less amount of oxidized copper (Cu(OH)$_2$ or CuO) in the thymine modified probe implies that the thymine molecules on top of the copper layer prevent the oxidation of copper adatoms during rinsing the sample with water and the transfer.

N-1s

For further information about the interactions between thymine molecules and the respective substrates, the N-1s signals were examined.

The first sample represents the chemisorbed thymine Au(111) electrode in the electrolyte containing 12 mM thymine at the emersion potential of 0.3 V. The N-1s signal obtained from this sample is shown in Fig. 6.9.a.

The second sample was prepared in the electrolyte containing 1 mM Cu(ClO$_4$)$_2$ and 12 mM thymine, waiting 10 minutes at the emersion potential of -0.48 V. The corresponding N-1s spectrum is presented in Fig. 6.9.b. Unfortunately, this spectrum has a poor signal to noise ratio compared to former one. Especially, the signal located around 399.75 eV is not so apparent. Therefore, the fitted peak in this spectrum does not recflect a well-defined signal. The interesting feature in this spectrum is that the weakness of the peak around 399.75 eV. Normally, this signal is close to the signal observed in multilayer thymine N(1) atom having almost no chemical interaction with surface gold atoms. Therefore, at some degree a downshift in the corresponding signal is possible upon interaction between Cu adatoms and thymine molecules.
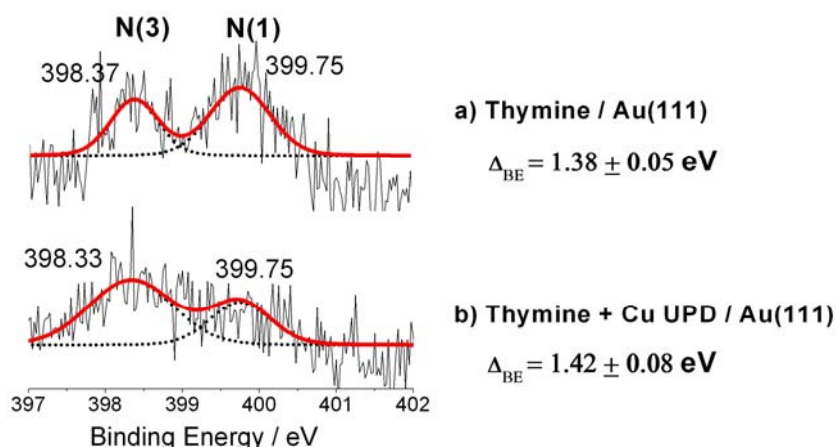
Both spectra have N-1s signals splitted into two components. These belong to the two nitrogen atoms existing in a thymine molecule, as notated by N(1) and N(3) (Fig.4.1). Normally, the XPS spectrum of multilayer thymine prepared in UHV has one single peak centered at 399.9 eV [14, 53, 110, 111]. After fitting the spectrum into two equal components having 1.1 eV FWHM, the separation between the peaks of the components was measured as 0.3 eV [111]. The poor peak separation of the two N atoms is due to their very similar chemical states. The curve centered at lower binding energies is related to N(3) according to ref. [53].

Comparing the spectra with the UHV spectrum [111] leads to the observation that there are shifts to lower binding energies for all chemisorbed samples. On the other hand, the difference in binding energy values (Δ_{BE}) of different nitrogen species is around 1.4 eV for the chemisorbed thymine on the bare Au(111) (a) and for the chemisorbed thymine Au(111)/Cu sample (b). This finding suggests that thymine and the substrate interact via the N(3), which confirms studies about thymine adsorption on Au(111) with SNIFTIRS experiments [26]. This may be achieved either by deprotonation leading to an increased electron density due to the lone pair at the N(3) as illustrated in Fig. 4.4 and Fig. 6.11.

C-1s

The first spectrum (Fig. 6.10.a) belongs to sample prepared in the electrolyte containing 12 mM thymine at the emersion potential of 0.3 V. The second spectrum (Fig.6.10.b) was obtained from the sample prepared in 12 mM thymine, 1 mM $Cu(ClO_4)_2$ and 0.1 M $HClO_4$ electrolyte waiting 10 minutes at the emersion potential of -0.48 V. The spectrum shown in Fig. 6.13.c is from the bare Au(111) sample which is flame annealed outside and transferred to the vacuum chamber. Hydrocarbon contamination is present in all spectra and contributes to a constant increase of the signal strength at 284-284.7 eV. This is due to the relatively long periods of the transfer and the measurement in UHV.
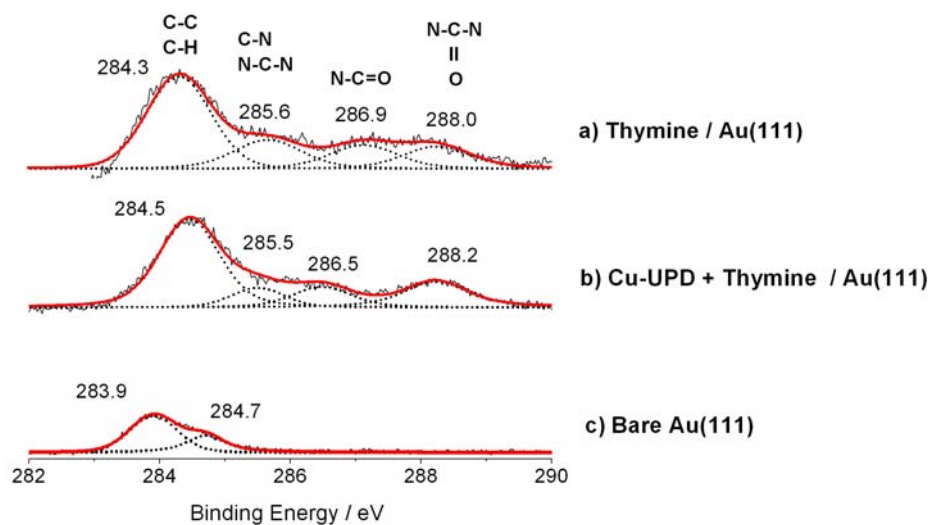
Figure 6.10: *C-1s spectra of chemisorbed thymine on bare Au(111) (**a**) chemisorbed thymine on Au(111) /(Cu UPD) (**b**) and bare Au(111) (**c**).*

The first two spectra are very similar each other. The carbon species expected from thymine include hydrocarbon (C-C and C-H), carbon bound to nitrogen (C-N, N-C-N), amide carbon (N-C=O), and urea carbon (N-C(=O)-N). These species have characteristic binding energies of approximately 285, 286-7, 288, and 289 eV, respectively [163]. This kind of carbon species are observed at both spectra (a) and (b). It obviously indicates that thymine is present on the bare Au(111) surface as well as on the underpotentially copper deposited Au(111).

6.1.4 The Mechanism of Supporting Effect of Thymine

When comparing the structure resolved by the *in situ* STM [7], chronocoulometric and *ex situ* XPS studies, it is reasonable to assume that copper adatoms on the Au(111) electrode are fully discharged and thymine molecules are chemisorbed on top of the copper layer at low underpotentials as illustrated in Fig. 6.11. The difference between the theoretical value of the charge which would be consumed if a full monolayer of neutral copper is formed (440 μCcm^{-2}) and the charge consumption calculated from the present chronocoulometric study (340-350 μCcm^{-2}) has its reason in the chemisorption of thymine molecules on top of the copper layer and the additional capacitive contribution.
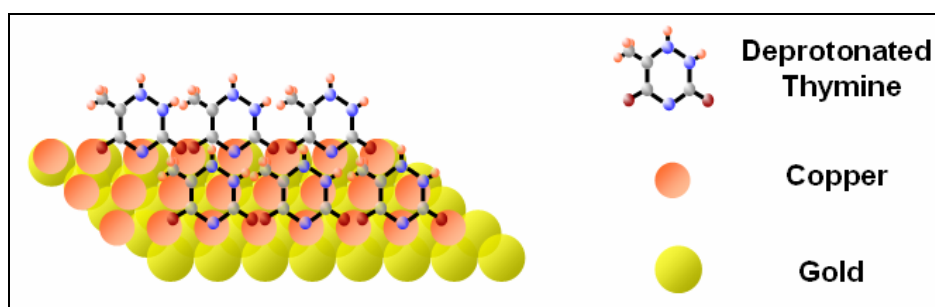
Figure 6.11: *The illustration of copper-thymine adlayer on top of gold atoms at lower underpotentials (-0.42 V).*

Summarizing, it can be stated that thymine molecules are upright oriented on Au(111) in the whole available potential region; at positive potentials on Au(111), at negative potentials on Au(111)/(Cu UPD). How can this effect be explained? The scheme shown Fig. 6.12 might help us to understand the mechanism. The potentials of zero charge (PZC) of Au(111) and Cu(111) in perchlorate solutions differ by about 380 mV. At potentials positive of the PZC Au(111), thymine is chemisorbed on top of the Au(111) substrate via N(3) atom. Negative of the PZC Au(111), thymine molecules are reorientated in a flat position on Au(111). At potentials at which the copper UPD starts the copper surface is simultaneously recharged from negative to positive values again and a change of the adsorption state of thymine from the physisorbed flat orientation on bare Au(111) to the chemisorbed upright orientation on copper occurs (again most likely via N(3) atom). This process takes place because the chemisorption on copper is more favoured than the physisorption on Au(111). But the supporting effect of thymine on copper in contrast to a pure perchlorate solution cannot be explained in this way. We speculate that the chemisorption of thymine on copper leads to a shift of the PZC (Cu) to more positive values reducing the interphase energy between the Au(111) substrate and the copper monolayer.
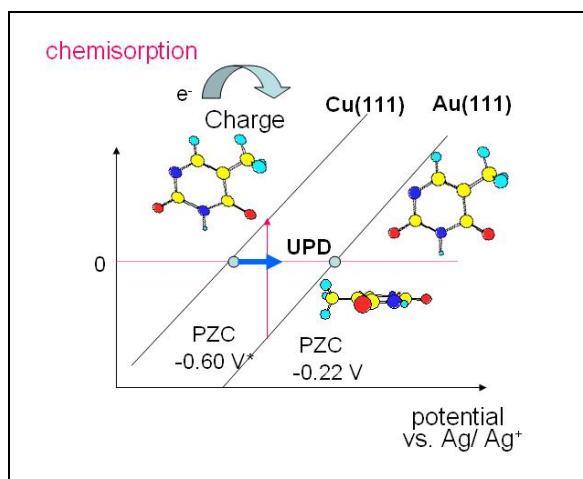
Figure 6.12: *The mechanism of the copper deposition on thymine modified Au(111).*

6.2 Adsorption behaviour of copper and thymine on Cu(111) electrode

The understanding of the adsorption behaviour of thymine on Au(111)/(Cu UPD) depends on the knowledge about the thymine adsorption on bulk copper surface. In order to investigate the interaction between thymine and bulk copper as well as the influence of thymine on the deposition of copper on Cu(111), we performed a series of electrochemical experiments.

To get a better quality of the surface we rinsed the crystal with a special solution of ammonia (25 %) and hydrogen peroxide (30 %) to remove the copper oxide layer at the surface. After rinsing with water, the (111) surface was polished onto the diamond polisher (1 μm) carefully and rinsed again with ultra pure water. Afterwards, the electrode was moved to the electrochemical cell for the experiment. Even though the reproducibility of results suggests accepting the convenience of the electrode, it is difficult to judge the quality of the surface because we could not flame anneal the surface of copper. Therefore, this electrode may have more lattice defects at the surface than the Au(111).

To observe some characteristic properties of the Cu(111) electrode, we examined it in 0.01 M $HClO_4$ electrolyte. The cyclic voltammogram measured at 5 mV/s scan rate and the corresponding capacity-potential curves are shown in Fig. 6.13. It is clear that the potential window of the Cu(111) electrode is narrow and locates at negative potentials compared to that of

Au(111) electrode. The minimum of the capacity-potential curves indicates the potential of zero charge which is about -0.6 V.
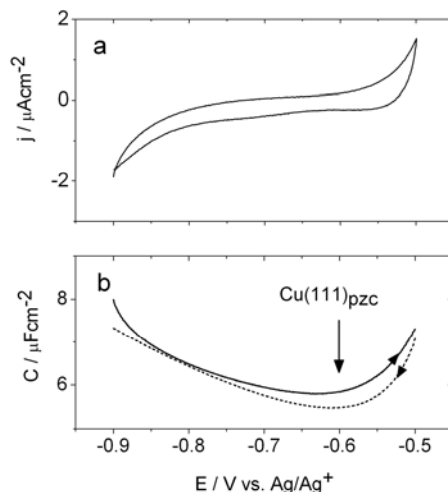
Figure 6.13.a: *The cyclic voltammogram of 0.01 M HClO₄ on Cu(111). Sweep rate: 5 mV/s.* ***b:*** *The corresponding capacity-potential curve. Perturbation frequency and amplitude: 200 Hz, and 3 mV, respectively.*

### 6.2.1 Deposition of copper on Cu(111): Influence of Anions

Anions influence the reduction of copper ions as shown in Fig. 6. 14. The Nernst potential for copper is -0.49 V vs. Ag/Ag$^+$ (0.1 M). The deposition of copper in the presence of perchlorate anion in the solution is strongly inhibited. However, in the electrolyte containing even only 1 mM CuSO₄ (supporting electrolyte contains perchlorate) copper deposition takes place around the Nernst potential. This behaviour is strange. It formally points to the adsorption of ClO$_4^-$ on the copper electrode negative of the PZC$_{Cu(111)}$. However, this obviously has not been studied so far.
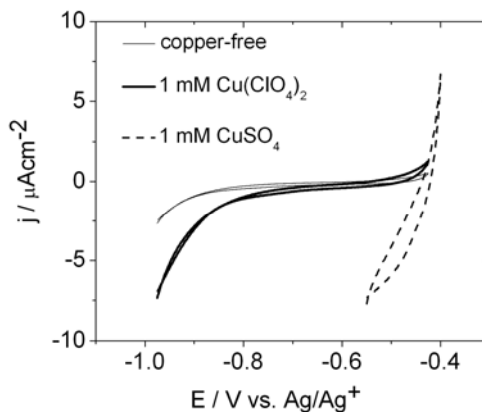
Figure 6.14: *The cyclic voltammograms on Cu(111) in 1 mM Cu(ClO$_4$)$_2$ (solid), 1 mM CuSO$_4$ (dashed) and without copper (thin) (supporting electrolyte: 0.100 M HClO$_4$ + 0.060 M NaClO$_4$). Sweep rates: 5 mV/s.*

6.2.2 Influence of thymine on the potential window of Cu(111) electrode

The following cyclic voltammograms in Fig. 6.15 show the influence of thymine on the oxidation and reduction of copper surface atoms. Electrolytes only contain 1 mM (thin curve) or 12 mM (thick curve) thymine within the supporting electrolyte of 0.100 M HClO$_4$ and 0.060 M NaClO$_4$. For comparison, the voltammogram of thymine-free electrolyte is included (dashed curve).
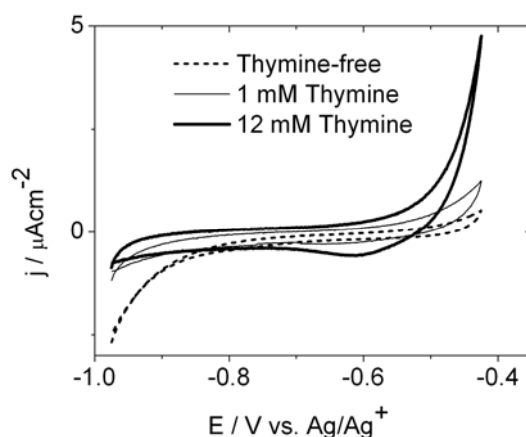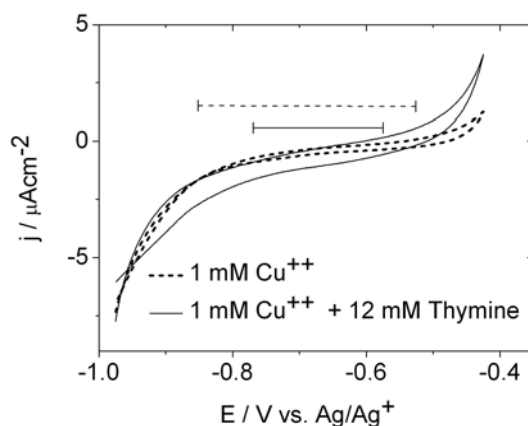

Figure 6.15: *The cyclic voltammograms on Cu(111) in 1 mM (thin) and 12 mM (solid) thymine concentrations (supporting electrolyte: 0.100 M HClO$_4$ + 0.060 M NaClO$_4$). Thymine free electrolyte is shown with dashed line. Sweep rate: 5 mV/s.*

It is clear that thymine inhibits the hydrogen evolution whereas interestingly supports the oxidation of the surface copper atoms. The degree of this effect strongly depends on the bulk concentration of thymine. This represents a different behaviour as compared to the Au(111) electrode where the oxidation of the gold surface atoms is strongly inhibited by the chemisorbed thymine.

6.2.3 Copper deposition on Cu(111) electrode in the presence of thymine

We examined the copper deposition on the Cu(111) electrode in the presence (12 mM, solid curve) and the absence (dashed curve) of thymine in 0.100 M HClO$_4$ and 0.06 M NaClO$_4$ electrolyte. The influence of thymine on the copper deposition is clearly seen in the voltammograms shown in Fig. 6.16. We already know from the former CV that thymine

molecules support the oxidation of copper surface atoms. It is interesting in the present CV that the reduction of copper ions in the solution containing thymine starts at more positive potentials compared to the reduction of copper in the absence of thymine. It shows that thymine molecules counteract against the inhibition of Cu^{++} reduction caused by ClO_4^-.

Figure 6.16: *The cyclic voltammograms on Cu(111) in 12 mM (solid) thymine + 1 mM Cu(ClO₄)₂ (solid) and in 1 mM Cu(ClO₄)₂ (dashed) electrolytes (supporting electrolyte: 0.1 M HClO₄ + 0.060 M NaClO₄). Sweep rates: 5 mV/s.*
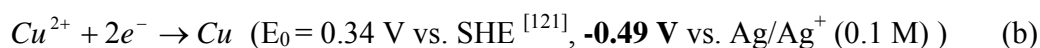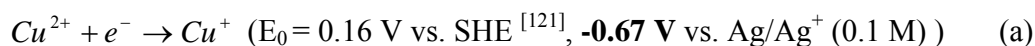
6.2.4 Possibility of copper-thymine complex

From the STM studies, we propose that the formation of a copper-thymine complex takes place at higher underpotentials (-0.31 V) on Au(111). We worked with the electrolyte containing 12 mM thymine with/without 1 mM Cu(ClO₄)₂ (supporting electrolyte: 0.100 M HClO₄, 0.060 M NaClO₄).
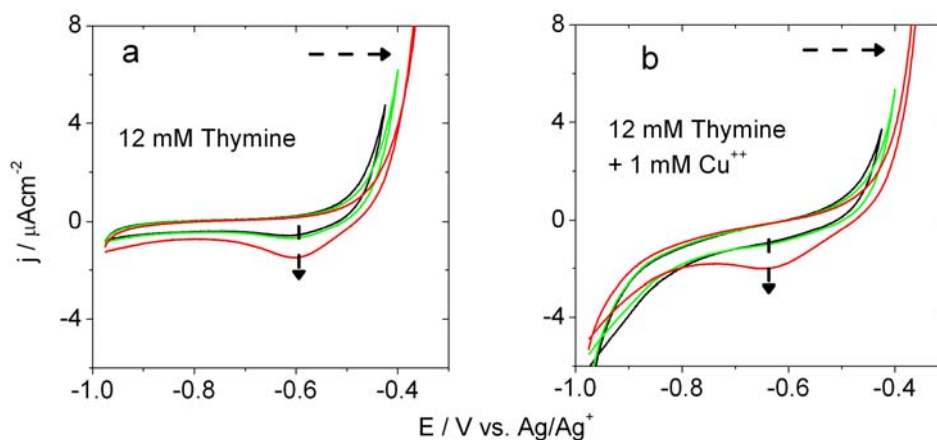
Figure 6.20: *The cyclic voltammograms obtained at increased cathodic potentials on Cu(111) in 12 mM thymine (**a**) and in 12 mM thymine + 1 mM Cu(ClO₄)₂ (**b**) electrolytes (supporting electrolyte: 0.100 M HClO₄ + 0.060 M NaClO₄). Sweep rate: 5 mV/s.*

During our studies on Cu(111), a small reduction wave is observed in the voltammograms (Fig. 6.20.a-b) when we scan to more positive potentials. We should remember that this kind of reduction peak is not observed in thymine-free electrolytes. The small wave, which depends not on the presence of copper ions in the electrolyte, implies the reduction of Cu^{2+} to Cu^{+}. In copper-free electrolyte (Fig. 6.20.a), the source of Cu^{2+} ions to be reduced is the oxidation of surface copper atoms. The standard redox potentials for 1 mM Cu^{2+} ions are as follow:

$$Cu^{2+} + e^{-} \rightarrow Cu^{+} \quad (E_0 = 0.16 \text{ V vs. SHE } [121], \textbf{-0.67 V} \text{ vs. Ag/Ag}^{+} \text{ (0.1 M)) } \quad (a)$$

$$Cu^{2+} + 2e^{-} \rightarrow Cu \quad (E_0 = 0.34 \text{ V vs. SHE } [121], \textbf{-0.49} \text{ V vs. Ag/Ag}^{+} \text{ (0.1 M)) } \quad (b)$$

The small reduction wave located between -0.5 V and -0.75 V most likely is related with the reaction a. Because this peak is observed in only thymine containing electrolytes, thymine must be involved in the reduction process. This can be possible as the reduction of copper-thymine complex as suggested in the following chemical reaction.

$$\left[Cu(thy)n\right]^{2+} + e^{-} \rightarrow \left[Cu(thy)n\right]^{+}$$
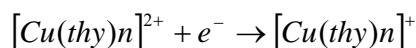
6.2.5 Summary

i)   The deposition of copper in the presence of ClO_4^{-} is strongly inhibited and takes place at ca. -0.3 V of the Nernst potential. However, the small amount of SO_4^{2-} in solution leads to copper deposition occurring around the Nernst potential.

ii)   Oxidation of Cu(111) surface atoms is supported by thymine. Contrarily, chemisorbed thymine molecules on Au(111) strongly inhibits the oxidation of surface atoms.

iii) Thymine molecules counteract against the inhibition of Cu^{++} reduction caused by ClO_4^{-}.

iv)   The reduction of the complex of $[Cu(thymine)_n]^{2+}$ to $[Cu(thymine)_n]^{+}$ on Cu(111) possibly takes place negative of the Nernst potential.

6.3 Copper Deposition on Adenine modified Au(111)

In addition to the study of copper deposition on the thymine modified Au(111) electrode, we examined the deposition of copper on the adenine modified Au(111) electrode. We already know that at negative potentials adenine molecules form charge transfer complexes having disordered and planar oriented structure on the Au(111) surface. At further positive potentials, a couple of broad ad- and desorption peaks, A_1/A_2 and A'_1/A'_2 (dissolution and formation of the charge transfer complex, respectively) followed by a chemisorbed and vertical orientated layer formation of adenine are observed (Fig. 6.17.a). The underpotential deposition of copper on the bare Au(111) electrode starts at the potential of -0.2 V whereby the formed charge transfer complex (vertical orientated) starts to dissolve and a physisorbed (tilted or parallel orientated) adenine layer is formed.
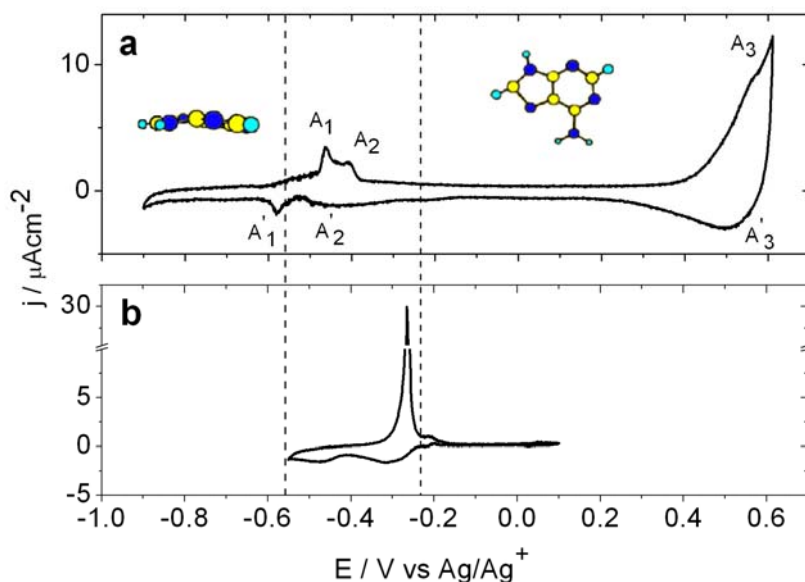
Figure 6.17: *The cyclic voltammograms of 2 mM Adenine (**a**) 1 mM Cu(ClO$_4$)$_2$ (**b**) on Au(111). Sweep rates: 50 mV/s (a) and 5 mV/s (b). 1 Supporting electrolyte: 0.1 M HClO$_4$ + 0.060 M NaClO$_4$).*

The following cyclic voltammograms scanned at 50 mV/s and 5 mV/s (Fig. 18.a-b) belong to the UPD of copper (1 mM Cu(ClO$_4$)$_2$) on Au(111) in the absence (dotted) and in the presence of 2 mM (thick) and 0.08 mM (thin) adenine (supporting electrolyte: 0.100 M HClO$_4$ and 0.060 M NaClO$_4$). In order to observe the influence of the adenine bulk concentrations on the the copper deposition, we have additionally chosen a lower concentration value of 0.08 mM adenine. We know that no significant difference is present between the voltammograms of higher and lower concentrated adenine on Au(111).
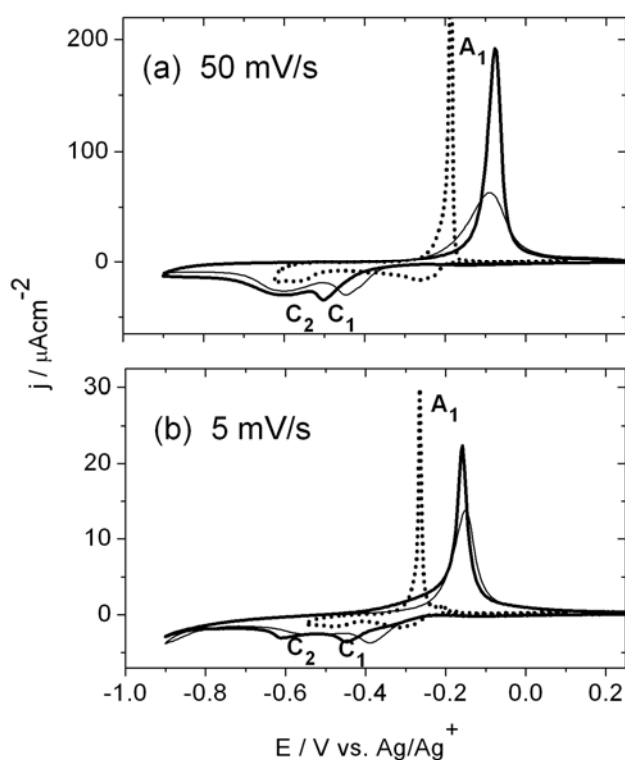
Figure 6.18: *Cyclic voltammograms on Au(111): Copper deposition (1 mM Cu(ClO$_4$)$_2$, without adenine (dot lines)), containing 2 mM adenine (thick lines), 0.08 mM adenine (thin lines) (supporting electrolyte: 0.1 M HClO$_4$ + 0.060 M NaClO$_4$). Scan rates: 50 (a), 5 mV/s (b).*

Similar to the thymine system, UPD of copper on adenine modified Au(111) electrode proceeds on two broad cathodic peaks (C$_1$, C$_2$) and a relatively sharp stripping peak (A$_1$). The inhibition of the first UPD peak is dominated at higher scan rate (a: 50 mV/s) compared to that of at lower rate (b: 5 mV/s). The positions of the pair of cathodic peaks are negatively shifted in the presence of the higher bulk concentration of adenine. It shows that the highly concentrated

adenine causes more inhibition against the UPD of copper around the first peak region. The second step of the copper deposition in the presence of adenine exhibits a similar behaviour like thymine. It is clear that adenine supports the UPD of copper at this step.

As similar to thymine, adenine also leads to the kinetic hindrance of the bulk deposition. The dissolution of the copper UPD layer is a one-step mechanism having a relatively sharp stripping peak, A_1. Beside this, the stripping peak of the UPD in the presence of concentrated adenine is sharper.

### 6.3.1 Chronocoulometry Experiments & *Avrami analysis*

In order to clarify the influence of adenine on the copper deposition on Au(111), we performed similar coulometric experiments done during the copper deposition on the thymine modified Au(111). We prepared copper (1 mM $Cu(ClO_4)_2$) electrolytes containing two different concentrations of 2 mM and 0.08 mM adenine in the supporting electrolyte of 0.100 M $HClO_4$, 0.060 M $NaClO_4$. The following potential sweep and step routine was applied:

i) Scanning from 0.3 V to the formation peak potentials (-0.465 V vs. Ag/Ag^+) with a scan rate of 2 mV/s and waiting there for different times.

ii) Stepping from the formation peak potential into the dissolution potential (0.1 V).

Dissolution process

The following dissolution transients and the corresponding Avrami analysis (Fig. 6.19) exhibit a different behaviour compared to the thymine-copper system (section 6.4.1). Despite the time scale of the dissolution is more or less the same with thymine system, the shapes of the transients are not so similar to the thymine results. The transients obtained in lower adenine concentration (0.08 mM Adenine, Fig. 6.19.b) upon waiting more than 8 minutes (blue and red curves) have sharper peaks and locate at lower times compared to that of having higher concentration of adenine (2 mM Adenine, Fig. 6.19.a). It implies that the influence of adenine on copper deposition gets smaller with lowering bulk concentration, or in other words, it resembles more to the behaviour of pure electrolyte (adenine-free, section 5.2.3.b). Actually, the result discussed here seems as a contradiction with reverse situation observed at the stripping peaks of voltammograms (Fig. 6.18) at first glance. However, this possibly points that the strength of

interaction (depending on the bulk adenine concentration) between copper adatoms and the adenine modified gold surface is weak (so, sharp stripping peak) at the early stages compared to the further ones.
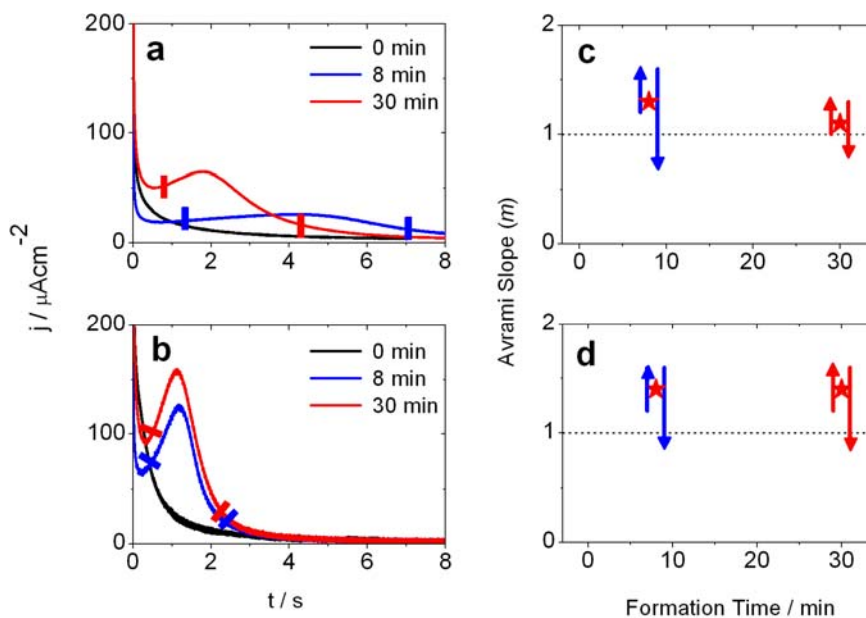
Figure 6.19: *Dissolution transients obtained after waiting at the formation potential of -0.465 V and stepping into the dissolution potential 0.1 V **a:** 2 mM adenine, **b:** 0.08 mM adenine in the electrolyte containing 1 mM $Cu(ClO_4)_2$, 0.1 M $HClO_4$, 0.060 M $NaClO_4$. **c-d:** The corresponding changes of Avrami slopes.*

The transients obtained without waiting (black curves) at the formation potential do not exhibit a minimum-maximum peak demonstrating the hole nucleation and growth mechanism. Therefore, for those transients overlapping of different processes, like diffusion controlled dissolution, is possible. The apperence of small peak in dissolution transients starts after waiting 2 minutes (not shown here) and grows depending on the waiting time at the formation potential. About this observation, the following can be proposed; at the beginning of deposition copper adatoms occupy the open places of adenine covered Au(111) surface. With further waiting, copper ions penetrate the adenine layer and adsorbed bottom of adenine molecules

The Avrami analysis for the transients having minimum-maximum peak (red and blue curves) were carried out considering the parts signed with rectangular shapes. The slope values of the Avrami plots change slightly over 1 for all considered transients. This reveals that an instantaneous hole nucleation combined with surface diffusion growth mechanism takes place

during dissolution process. It should be remembered that the slopes observed in thymine-copper system are very high (*m*: 4-15).

From the Predator-prey point of view, an increase and decrease in Avrami slopes are observed as before.

Charge density diagram

The integration of the dissolution transients results in the charge–potential diagram shown in Fig. 6.20. For a better comparison, the diagram obtained from pure electrolyte (adenine-free, section 5.2.3.b) is included (full-circle).
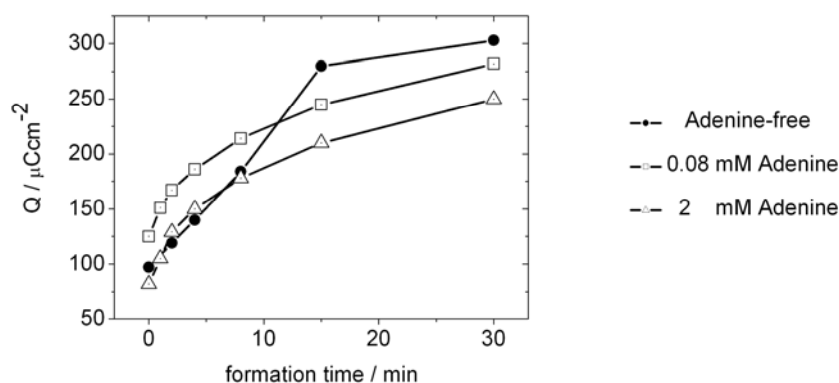
Figure 6.20: *Charge values obtained after the integration of the dissolution transients.* **triangle:** *2 mM adenine / copper,* **square:** *0.08 mM adenine / copper,* **full circle:** *copper (from section 5.2.3.b).*

It is clear that the charge evolution with the waiting time at the formation potential is different from that of thymine-copper system. In comparison to the charge diagram of pure electrolyte (full circle), adenine containing electrolytes inhibit the copper deposition at the overall time scale depending on the bulk concentration. The exception occurs during the first 8 minutes of waiting time in the electrolyte containing lower concentration of adenine (0.08 mM Adenine, square) that the charge values are higher than others. In contrast to the thymine-copper system, less charge is evolved in the presence of higher bulk concentration of adenine. At the end of waiting half an hour at the formation potential, the charge values of 282 ± 7 μCcm^{-2} and 250 ± 7 μCcm^{-2} are accumulated 0.08 mM and 2 mM adenine containing solutions, respectively. The large charge density deficiency compared to the theoretical value (440 μCcm^{-2}) implies two possibilities (Fig. 6.21);

A) Adenine may posses a direct interaction with the Au(111) surface, therefore, it limitates the number of fully reduced deposited copper, or

B) Adenine may not have direct interaction with gold atoms, but, copper adatoms under adenine molecules are not fully discharged (copper-adenine complex). By this representation, N(7) and C(8) atoms of adenine can form a complex with Cu as also proposed by Masoud et. al.[164] in solution phase.
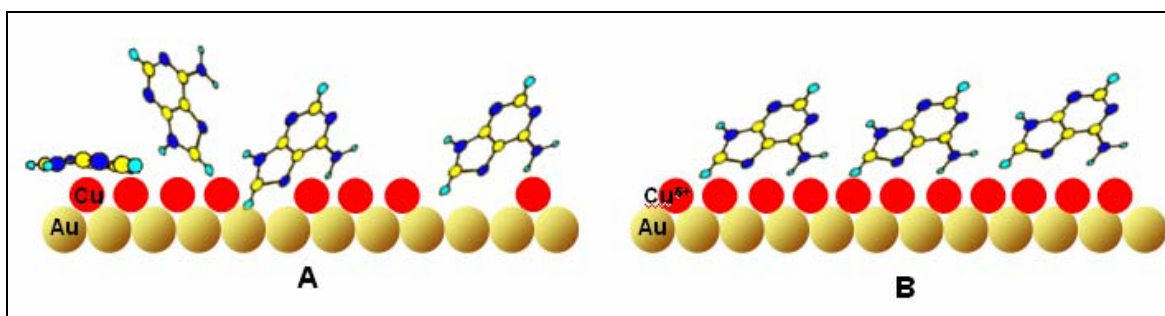
Figure 6.21: *Schematic representations of adenine-copper adlayers.*

6.3.2 Comparison of cyclic voltammograms of adenine and thymine

Above, in the part of copper deposition on the adenine modified Au(111), the comparison of thymine and adenine results have been made at some points. Besides these, the following CVs (Fig. 6.22) help us to compare the adsorption behaviour of the modified and unmodified systems. The voltammograms taken at two different sweep rates (a: 50 mV/s, b: 5 mV/s) were obtained from the 2 mM adenine (thick curves) and 12 mM thymine (thin curves) containing electrolytes in the presence of 1 mM $Cu(ClO_4)_2$, 0.1 M $HClO_4$, 0.060 M $NaClO_4$. The dashed curves belong to the copper UPD on the unmodified electrode.
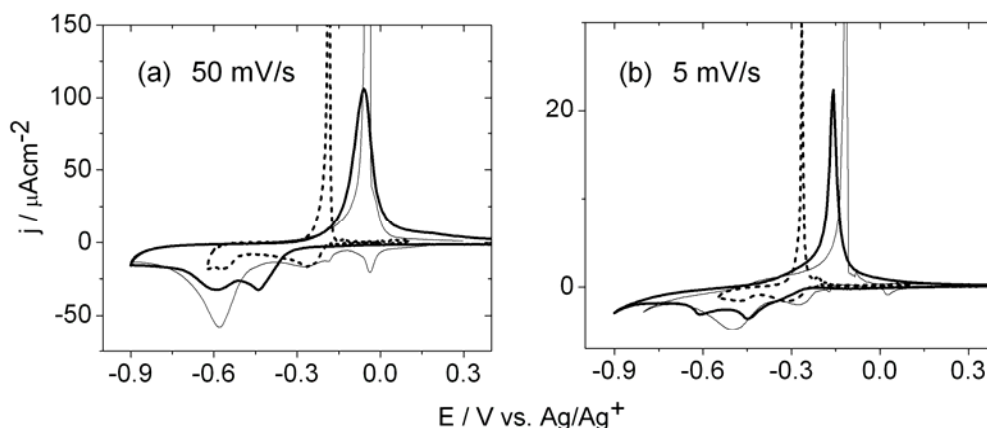
Figure 6.22: *Cyclic voltammograms on Au(111): Copper deposition (1 mM Cu(ClO$_4$)$_2$, without adenine or thymine (dashed lines)), containing 2 mM adenine (thick lines), 12 mM thymine (thin lines) (supporting electrolyte: 0.100 M HClO$_4$ + 0.060 M NaClO$_4$). Scan rates: 50 (a), 5 mV/s (b).*

At these voltammograms, the influence of adenine on the deposition of copper on Au(111) seems to be similar to that of thymine. At first glance, the supporting effect of adenine to the UPD of copper can be claimed due to the higher cathodic peaks compared to the unmodified one. However, it occurs slightly only at the initial stages (0-8 minutes) of deposition because, the results obtained from coulometry (Fig. 6.20) indicates the presence of inhibition at larger time scale. The stripping peaks locate almost at the same potential. It reveals that the strengths of copper adatom adsorption is probably close each other. However, in adenine containing electrolyte this peak is smaller but broader than that of thymine containing one. It shows that the formed copper-thymine adlayer on Au(111) has a more uniform structure compared to the copper-adenine one.

6.3.3 Summary

i)   At the early stage of Cu-UPD is supported slightly in adenine containing electrolyte compared to that in pure one. However, at further stages adenine inhibits the UPD at a low degree.

ii)   The higher strength of the interaction between charge-transferred adenine complex and gold surface atoms leads to the inhibition.

iii) The degree of inhibition rises with bulk concentration of adenine.

iv)   The dissolution process exhibits a hole nucleation and growth mechanism in the samples adjusted some time at the formation potential.